

RAIN STREAKS REMOVAL FOR SINGLE IMAGE VIA DIRECTIONAL TOTAL VARIATION REGULARIZATION

Yugang Wang, Ting-Zhu Huang, Xi-Le Zhao, Liang-Jian Deng, Tai-Xiang Jiang

School of Mathematical Sciences/Research Center for Image and Vision Computing,
University of Electronic Science and Technology of China, Chengdu, Sichuan, 611731, P. R. China.

ABSTRACT

Images captured in rainy conditions are often corrupted by unexpected rain streaks, which severely degrade the performance of subsequent processes in outdoor computer vision systems. In this paper, we exploit the directional smoothness of rain streaks for the single-image rain streaks removal and propose a convex model that uses the directional total variation (DTV) to characterize the smoothness of rain streaks in arbitrary orientations. The proposed model consists of four terms: the fidelity term, the ℓ_1 norm for the sparsity of rain streaks, and two DTV regularization terms for the directional smoothness and the piecewise smoothness of rain streaks and rain-free backgrounds, respectively. To solve the proposed model, we develop an efficient algorithm based on the alternating direction method of multipliers (ADMM) framework. Extensive experimental results on both synthetic and real rainy images show that our method outperforms the recent state-of-the-art methods visually and quantitatively.

Index Terms— Single-image rain streaks removal, directional total variation (DTV), alternating direction method of multipliers

1. INTRODUCTION

Outdoor images taken in rainy weather usually suffer from the undesirable interference caused by the inevitable falling raindrops. The captured rain images often contain bright rain streaks which may obstruct the background [1], distort the colors, and blur the true scenes. These types of visibility degradation would severely affect the performance of many algorithms in outdoor computer vision systems. Thus the removal of rain streaks is an essential and urgent issue and has received much attention in recent years.

Garg *et al.* [2, 3] first proposed to detect and remove the rain streaks from videos by adopting the photometric appearance of raindrops or altering camera settings. In the last few

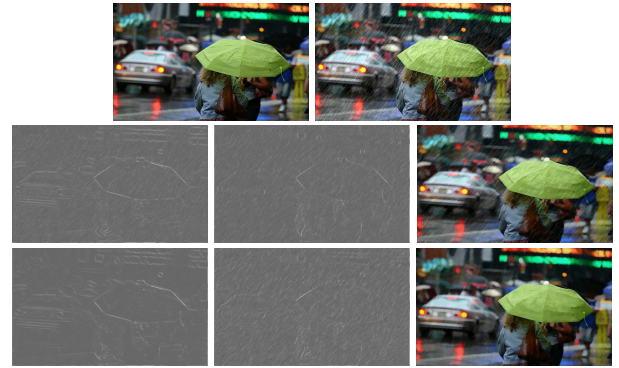


Fig. 1. The first row shows a rain-free image and its simulated rainy image with oblique rain streaks. The second row shows the vertical derivative of the rainy image, the horizontal derivative of the rainy image, and the recovered image using the vertical smoothness of rain streaks. The last row shows the derivative along the rain direction, the derivative along the rain-perpendicular direction, and the recovered image using the rain directional smoothness via DTV.

decades, abundant literatures aimed at video rain streaks removal using the spatial-temporal redundancy of videos [4, 5]. Comparing with removing rain from videos, single image rain streaks removal is a more challenging task since only one rainy frame is given. To effectively estimate the rain-free content from a rainy image, many existing methods had explored various priors for both rain streaks and rain-free backgrounds and achieved impressive results. The dictionary-based sparse prior [6–8] was used via finding the discriminative sparse representations of clean images or rain streaks under the given or learned dictionary. Chen *et al.* [9] leveraged a low-rank prior for the rain streaks patches. Kim *et al.* [10] and Chang *et al.* [11] incorporated the nonlocal self-similarity property into their rain removal methods. Li *et al.* [1] removed the rain streaks using Gaussian Mixed Model (GMM) to characterize the rain layer. The methods based on deep networks were recently proposed for the deraining task by learning deep features of both rain streaks and clean images [12–16]. Some approaches [17–19] took the directional smooth property of

This research is supported by NSFC (61772003, 61876203, 61702083), Science Strength Promotion Programme of UESTC, and the Fundamental Research Funds for the Central Universities (ZYGX2016J132, ZYGX2016KYQD142).

rain streaks into account. These methods assumed the rain direction to be vertical and used the unidirectional total variation to characterize the directional smoothness of rain streaks. However, in most real-world applications, images are often corrupted by oblique rain streaks so that the vertical smoothness of rain streaks would not be satisfied (see Fig. 1). Even though Deng *et al.* [17] handled the oblique rain streaks by rotating the image to get the vertical rain streaks, the operations of rotation often cause the resampling of image pixels and inevitable degrade the images.

To dealing with the oblique rain streaks in more general case, in this paper, we employ the directional total variation (DTV) regularization, which can characterize the directional smoothness in arbitrary directions, to regularize the oblique rain streaks and the rain-free backgrounds. The contributions of this paper can be summarized as follows:

- We consider the directional smoothness of oblique rain streaks, and propose a convex model utilizing DTV to characterize the smoothness of rain streaks in arbitrary directions. To the best of our knowledge, our work is the first attempt to bring DTV regularization in rain streaks removal task.
- To tackle the proposed model, we develop an efficient algorithm based on the alternating direction method of multipliers (ADMM) framework where the convergence can be theoretically guaranteed. Extensive experiments demonstrate the superiority of our method visually and quantitatively.

The rest of this paper is organized as follows. In Section 2, we introduce the DTV and present the proposed method. Section 3 shows the experimental results on both synthetic and real rain images. The conclusion is given in Sectoin 4.

2. RAIN STREAKS REMOVAL VIA DTV REGULARIZATION

2.1. Directional Total Variation

We define ∇_1 and $\nabla_2: \mathbb{R}^{m \times n} \rightarrow \mathbb{R}^{m \times n}$ as the first-order difference operator, respectively, along horizontal and vertical directions with circulant boundary condition. Then for a discrete-space image $\mathbf{X} \in \mathbb{R}^{m \times n}$, the directional total variation (DTV) [20, 21] of \mathbf{X} can be formulated as

$$\text{DTV}_{\theta,a}(\mathbf{X}) = \sum_{i,j} \|\tilde{\nabla}_{\theta,a}\mathbf{X}(i,j)\|_2, \quad (1)$$

where $a \in [0, 1]$ is a positive parameter and $0 < \theta < 180^\circ$ can be an arbitrary direction. $\tilde{\nabla}_{\theta,a}\mathbf{X}(i,j)$ can be written as

$$\tilde{\nabla}_{\theta,a}\mathbf{X}(i,j) = \Lambda_a R_{-\theta} \begin{pmatrix} \nabla_1 \mathbf{X}(i,j) \\ \nabla_2 \mathbf{X}(i,j) \end{pmatrix}, \quad (2)$$

where

$$\Lambda_a = \begin{pmatrix} 1 & 0 \\ 0 & a \end{pmatrix}, R_{-\theta} = \begin{pmatrix} \cos \theta & \sin \theta \\ -\sin \theta & \cos \theta \end{pmatrix} \quad (3)$$

are the translation matrix and rotation matrix, respectively. The DTV has been widely used for modeling the images whose texture mainly has one direction θ in image restoration literatures [20, 21]. Form Fig. 1, we can observe that the vertical gradient failes to model the oblique rain streaks, while DTV can effectively characterize the directional smoothness and recover the better rain-free background.

2.2. The Proposed Model for Rain Streaks Removal

The degradation model [1] of a rainy image can be written as

$$\mathbf{O} = \mathbf{B} + \mathbf{R}, \quad (4)$$

where \mathbf{O} , \mathbf{B} , and $\mathbf{R} \in \mathbb{R}^{m \times n}$ are the observed rain image, the desired clean image, and the rain streaks layer, respectively. To recover \mathbf{B} from \mathbf{O} , we use the DTV regularizer to characterize the directional smoothness of \mathbf{R} . In addition, an ℓ_1 norm is also utilized to enhance the sparsity of rain streaks. To model the clean background \mathbf{B} , we consider the piecewise smoothness of natural images and also utilize the the DTV regularization for \mathbf{B} along rain-perpendicular direction. Thus, the proposed model can be formulated as follows

$$\begin{aligned} \min_{\mathbf{O}, \mathbf{R}} \quad & \frac{1}{2} \|\mathbf{O} - \mathbf{B} - \mathbf{R}\|_F^2 + \lambda_1 \sum_{i,j} \|\tilde{\nabla}_{\theta,a_1} \mathbf{R}(i,j)\|_2 \\ & + \lambda_2 \|\mathbf{R}\|_1 + \lambda_3 \sum_{i,j} \|\tilde{\nabla}_{\theta^\perp,a_2} \mathbf{B}(i,j)\|_2 \\ \text{s.t.} \quad & 0 \leq \mathbf{B} \leq \mathbf{O}, 0 \leq \mathbf{R} \leq \mathbf{O}, \end{aligned} \quad (5)$$

where θ is the rain direction and $\theta^\perp = \theta + 90^\circ$ is the orthogonal direcion of θ . λ_1 , λ_2 , and λ_3 are positive parameters. In the next section, we develop an efficient algorithm based on ADMM framework [22] to solve this proposed model.

2.3. The Numerical Algorithm

Based on the ADMM principle, we introduce several auxiliary variables and set the constraints $(\mathbf{U}_1^\top, \mathbf{U}_2^\top)^\top = \tilde{\nabla}_{\theta,a_1} \mathbf{R}$, $(\mathbf{M}_1^\top, \mathbf{M}_2^\top)^\top = \tilde{\nabla}_{\theta^\perp,a_2} \mathbf{B}$, $\mathbf{V} = \mathbf{R}$, $\mathbf{P} = \mathbf{R}$ and $\mathbf{Q} = \mathbf{B}$. Then the augmented Lagrangian function of (5) can be written as

$$\begin{aligned} \mathcal{L}(\Phi, \mathbf{\Gamma}_1, \mathbf{\Gamma}_2, \mathbf{\Gamma}_3, \mathbf{K}_2, \mathbf{K}_2, \mathbf{L}_1, \mathbf{L}_2) = & \\ & \frac{1}{2} \|\mathbf{O} - \mathbf{B} - \mathbf{R}\|_F^2 + \lambda_1 \sum_{i,j} \|(\mathbf{U}_1(i,j), \mathbf{U}_2(i,j))^\top\|_2 \\ & + \lambda_2 \|\mathbf{V}\|_1 + \lambda_3 \sum_{i,j} \|(\mathbf{M}_1(i,j), \mathbf{M}_2(i,j))^\top\|_2 \\ & + \frac{\beta}{2} \|(\mathbf{U}_1^\top, \mathbf{U}_2^\top)^\top - \tilde{\nabla}_{\theta,a_1} \mathbf{R} + \frac{1}{\beta} (\mathbf{K}_1^\top, \mathbf{K}_2^\top)^\top\|_F^2 \end{aligned}$$

$$\begin{aligned}
& + \frac{\beta}{2} \|(\mathbf{M}_1^\top, \mathbf{M}_2^\top)^\top - \tilde{\nabla}_{\theta^\perp, a_2} \mathbf{B} + \frac{1}{\beta} (\mathbf{L}_1^\top, \mathbf{L}_2^\top)^\top\|_F^2 \\
& + \frac{\beta}{2} \|\mathbf{V} - \mathbf{R} + \frac{1}{\beta} \mathbf{\Gamma}_1\|_F^2 + \frac{\beta}{2} \|\mathbf{P} - \mathbf{R} + \frac{1}{\beta} \mathbf{\Gamma}_2\|_F^2 \\
& + \frac{\beta}{2} \|\mathbf{Q} - \mathbf{B} + \frac{1}{\beta} \mathbf{\Gamma}_3\|_F^2 + \rho(\mathbf{P}) + \rho(\mathbf{Q}),
\end{aligned} \quad (6)$$

where $\Phi = \{\mathbf{B}, \mathbf{R}, \mathbf{U}_1, \mathbf{U}_2, \mathbf{M}_1, \mathbf{M}_2, \mathbf{P}, \mathbf{V}, \mathbf{Q}\}$ is the set of variables, $\mathbf{K}_1, \mathbf{K}_2, \mathbf{L}_1, \mathbf{L}_2, \mathbf{\Gamma}_1, \mathbf{\Gamma}_2, \mathbf{\Gamma}_3$ are the Lagrangian multipliers and β is a positive scalar. $\rho(\cdot)$ is the indicator function defined as

$$\rho(\mathbf{X}(i, j)) = \begin{cases} 0, & 0 \leq \mathbf{X}(i, j) \leq \mathbf{O}(i, j), \\ +\infty, & \text{otherwise.} \end{cases} \quad (7)$$

The sub-problems of $(\mathbf{U}_1^\top, \mathbf{U}_2^\top)^\top$ and $(\mathbf{M}_1^\top, \mathbf{M}_2^\top)^\top$ have closed-form solutions which can be calculated by the shrinkage formula [22]

$$\begin{aligned}
\left(\begin{array}{c} \mathbf{U}_1^{k+1}(i, j) \\ \mathbf{U}_2^{k+1}(i, j) \end{array} \right) &= \max \left(\left\| \mathbf{d}_{ij}^k \right\|_2 - \frac{\lambda_1}{\beta}, 0 \right) \frac{\mathbf{d}_{ij}^k}{\left\| \mathbf{d}_{ij}^k \right\|_2}, \\
\left(\begin{array}{c} \mathbf{M}_1^{k+1}(i, j) \\ \mathbf{M}_2^{k+1}(i, j) \end{array} \right) &= \max \left(\left\| \mathbf{w}_{ij}^k \right\|_2 - \frac{\lambda_3}{\beta}, 0 \right) \frac{\mathbf{w}_{ij}^k}{\left\| \mathbf{w}_{ij}^k \right\|_2},
\end{aligned}$$

where \mathbf{d}_{ij}^k and \mathbf{w}_{ij}^k are vectors defined as

$$\begin{aligned}
\mathbf{d}_{ij}^k &= \tilde{\nabla}_{\theta, a_1} \mathbf{R}^k(i, j) - \frac{1}{\beta} (\mathbf{K}_1^k(i, j), \mathbf{K}_2^k(i, j))^\top, \\
\mathbf{w}_{ij}^k &= \tilde{\nabla}_{\theta^\perp, a_2} \mathbf{B}^k(i, j) - \frac{1}{\beta} (\mathbf{L}_1^k(i, j), \mathbf{L}_2^k(i, j))^\top.
\end{aligned} \quad (8)$$

The variable \mathbf{V} can be solved by a shrinkage operator

$$\mathbf{V}^{k+1}(i, j) = \text{shrink}(\mathbf{R}^k(i, j) - \frac{\mathbf{\Gamma}_1^k(i, j)}{\beta}, \frac{\lambda_2}{\beta}), \quad (9)$$

where **shrink** is the soft-shrinkage operator [23].

\mathbf{P}^{k+1} and \mathbf{Q}^{k+1} can be respectively updated by projecting $\mathbf{R}^k - 1/\beta \mathbf{\Gamma}_2^k$ and $\mathbf{B}^k - 1/\beta \mathbf{\Gamma}_3^k$ between 0 and \mathbf{O} .

\mathbf{B} and \mathbf{R} should be jointly solved. Their sub-problem is a least squares problem which could be efficiently solved by fast Fourier transforms (FFTs) and Cramer's rule [24].

At last, each Lagrangian multiplier are updated by gradient ascent optimization with the other variables fixed [22].

We set $a_1 = 0$ and $a_2 = 0.5$ in all experiments. To estimate the rain direction θ , we employ the strategy of [25] to first search the rain-dominated patches of a rain image, which contain little background details. Then we find the directions in which the smallest DTV values of these rain-dominated patches can be achieved. At last, we calculate the average of these directions to approximate θ .

3. EXPERIMENTAL RESULTS

In this section, we test our method on both synthetic and real-world rainy images. Three state-of-the-art methods: GMM

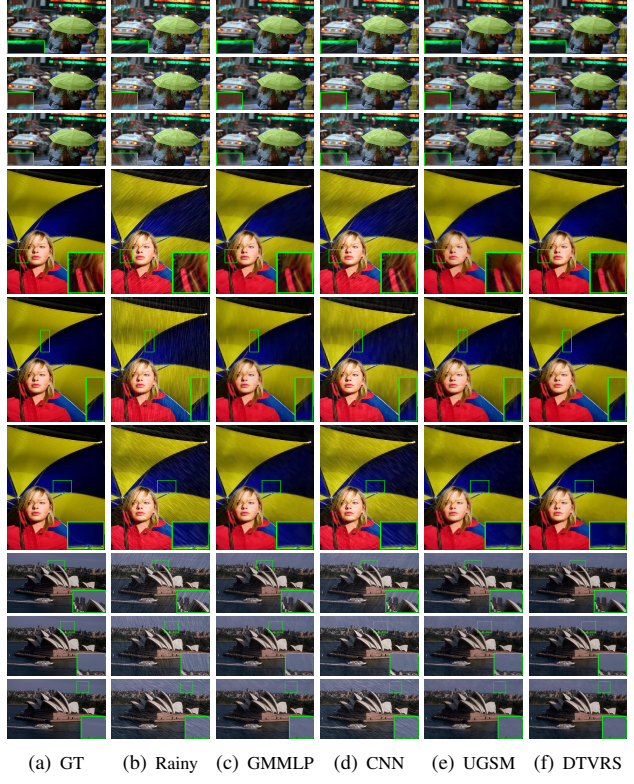


Fig. 2. The visual comparison on three images with different rain directions.

layer prior (GMMLP) based method [1], convolutional neural network (CNN) method [26], and the unidirectional global sparse method (UGSM) [17] are compared with the proposed DTV regularized sparse (DTVRS) method. All experiments are implemented in MATLAB 2017b on an Intel 3.70 GHz PC with 16GB RAM, and a GTX1060 GPU. We efficiently implement DTVRS on the GPU device. The computing time for our method is about 14 seconds for running a color image of size $366 \times 550 \times 3$.

3.1. Synthetic Experiments

We generate the synthetic rain streaks using the same strategy as [18], which first adds the “salt and pepper” noise on a zero image and then convolutes it with a motion blur kernel to form the rain streaks. The density of “salt and pepper” noise is taken randomly in the range of [0.05, 0.1] and the length of motion is set in [10, 30]. Empirically, we set $\beta = 0.1$, and select λ_1, λ_2 , and λ_3 in the sets of {0.1, 0.2}, {0.001, 0.002, 0.003}, and {0.02, 0.03, 0.04}, respectively. For quantitative assessment, the peak signal-to-noise ratio (PSNR) and the structural similarity (SSIM) are calculated for all the result images.

We firstly adopt three nature images named “umbrella”, “girl”, and “Sydney” which are widely used in image derain-

Table 1. Quantitative evaluation on synthetic images with rain streaks of different directions.

	Images	umbrella			girl			Sydney		
Directions	θ^*	30°	75°	120°	45°	90°	135°	60°	105°	150°
	θ	27.6°	76.2°	121.2°	45°	90°	135.6°	51.2°	112.6°	148.4°
PSNR	Rainy	23.8405	26.0357	23.8180	25.2197	24.8202	24.9191	23.8766	23.9786	23.4225
	GMMLP	29.4895	31.5672	29.4545	31.8517	33.4776	32.3116	29.5498	29.8990	29.6320
	CNN	24.1248	27.2630	24.3583	25.6772	26.6789	25.4605	24.3659	24.5482	23.6691
	UGSM	28.6841	30.8983	29.0354	28.9564	33.3201	29.3947	28.0436	29.9268	27.3833
	DTVRS	31.3372	32.2719	32.0719	35.0720	33.5534	30.7475	32.4554	32.3067	31.5733
SSIM	Rainy	0.7978	0.8481	0.8019	0.8749	0.8598	0.8676	0.8154	0.8113	0.7833
	GMMLP	0.9413	0.9506	0.9424	0.9464	0.9599	0.9503	0.9279	0.9276	0.9202
	CNN	0.8206	0.9328	0.8533	0.8847	0.9060	0.8792	0.8611	0.8974	0.8027
	UGSM	0.9287	0.9552	0.9359	0.9536	0.9722	0.9491	0.9067	0.9234	0.8758
	DTVRS	0.9477	0.9552	0.9547	0.9800	0.9718	0.9739	0.9356	0.9345	0.9252

Table 2. Quantitative evaluation on BSD500 dataset.

Metrics	rainy	GMMLP	CNN	UGSM	DTVRS
PSNR	23.7936 ± 1.1749	28.4303 ± 1.4479	24.2219 ± 1.2437	26.1925 ± 2.0719	29.3313 ± 1.7251
SSIM	0.8405 ± 0.0690	0.9259 ± 0.0326	0.8675 ± 0.0580	0.8966 ± 0.0435	0.9306 ± 0.0291

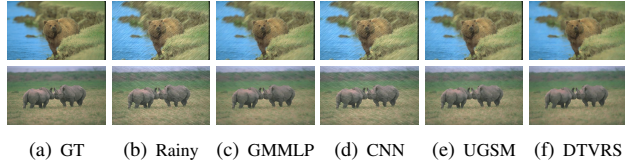


Fig. 3. The visual comparison on two synthetic rain images of BSD500 dataset.

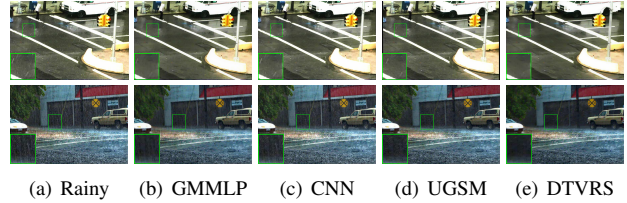


Fig. 4. The visual comparison on two real-world rain images.

ing literatures [1, 17, 25]. To test the performance on various directional rain streaks, we simulate the rain streaks with 9 different directions that are from 30° to 150° with step size 15° . Fig. 2 shows the visual performance of different approaches. We can see that the proposed DTVRS outperforms the other compared methods in both rain streaks removal and background details recovery. Table 1 shows the quantitative results. The ground truth and estimated rain direction are denoted as θ^* and θ , respectively. Since UGSM also requires the rain direction when dealing with oblique rain streaks, we input the estimated θ for UGSM for fair comparison. Table 1 demonstrates that DTVRS achieves the best PSNR and SSIM for most of all cases.

We also test all the methods on 60 images from BSD500 dataset [27] with arbitrary rain directions simulated from 20° to 160° . Fig. 3 and Table 2 respectively show the visual comparison of two selected images and the mean measurements of 60 images, which illustrate the superiority of the proposed DTVRS for the deraining task.

3.2. Real Experiments

In this section, we test all the methods on two real images. One image is corrupted by oblique light rain and another contains heavy rain in nearly vertical direction. Fig. 4 shows the visual comparison results. We can observe that some shadow rain streaks (in the first row) or dense rain streaks (in the second row) are not removed completely by the other compared methods. While our method removes most of the rain streaks and recovers the rain-free background successfully.

4. CONCLUSION

In this paper, we addressed the single-image deraining task by exploiting the directional smoothness of rain streaks in arbitrary directions. We proposed a convex model using DTV to characterize the discriminative smoothness of rain streaks and rain-free backgrounds, respectively. To solve the proposed model, we developed an efficient algorithm based on ADMM framework. Extensive experimental results demonstrate the superiority of our method visually and quantitatively.

5. REFERENCES

- [1] Y. Li, R. T. Tan, X. Guo, J. Lu, and M. S. Brown, “Rain streak removal using layer priors,” in *2016 IEEE Conference on Computer Vision and Pattern Recognition (CVPR)*, June 2016, pp. 2736–2744.
- [2] K. Garg and S. K. Nayar, “Detection and removal of rain from videos,” in *2004 IEEE Conference on Computer Vision and Pattern Recognition (CVPR)*, June 2004, vol. 1, pp. I–I.
- [3] K. Garg and S. K. Nayar, “When does a camera see rain?,” in *2005 IEEE International Conference on Computer Vision (ICCV)*, Oct 2005, vol. 2, pp. 1067–1074.
- [4] M. Li, Q. Xie, Q. Zhao, W. Wei, S. Gu, J. Tao, and D. Meng, “Video rain streak removal by multiscale convolutional sparse coding,” in *2018 IEEE Conference on Computer Vision and Pattern Recognition (CVPR)*, June 2018, pp. 6644–6653.
- [5] J. Liu, W. Yang, S. Yang, and Z. Guo, “D3r-net: Dynamic routing residue recurrent network for video rain removal,” *IEEE Transactions on Image Processing*, vol. 28, no. 2, pp. 699–712, Feb 2019.
- [6] L. Kang, C. Lin, and Y. Fu, “Automatic single-image-based rain streaks removal via image decomposition,” *IEEE Transactions on Image Processing*, vol. 21, no. 4, pp. 1742–1755, April 2012.
- [7] Y. Luo, Y. Xu, and H. Ji, “Removing rain from a single image via discriminative sparse coding,” in *2015 IEEE International Conference on Computer Vision (ICCV)*, Dec 2015, pp. 3397–3405.
- [8] L. Kang, C. Lin, C. Lin, and Y. Lin, “Self-learning-based rain streak removal for image/video,” in *2012 IEEE International Symposium on Circuits and Systems*, May 2012, pp. 1871–1874.
- [9] Y. Chen and C. Hsu, “A generalized low-rank appearance model for spatio-temporally correlated rain streaks,” in *2013 IEEE International Conference on Computer Vision (ICCV)*, Dec 2013, pp. 1968–1975.
- [10] J. Kim, C. Lee, J. Sim, and C. Kim, “Single-image deraining using an adaptive nonlocal means filter,” in *2013 IEEE International Conference on Image Processing*, Sept 2013, pp. 914–917.
- [11] Y. Chang, L. Yan, and S. Zhong, “Transformed low-rank model for line pattern noise removal,” in *2017 IEEE International Conference on Computer Vision (ICCV)*, Oct 2017, pp. 1735–1743.
- [12] H. Zhang and V. M. Patel, “Convolutional sparse and low-rank coding-based rain streak removal,” in *2017 IEEE Winter Conference on Applications of Computer Vision (WACV)*, March 2017, pp. 1259–1267.
- [13] X. Fu, J. Huang, D. Zeng, Y. Huang, X. Ding, and J. Paisley, “Removing rain from single images via a deep detail network,” in *2017 IEEE Conference on Computer Vision and Pattern Recognition (CVPR)*, July 2017, pp. 1715–1723.
- [14] H. Zhang and V. M. Patel, “Density-aware single image de-raining using a multi-stream dense network,” in *2018 IEEE Conference on Computer Vision and Pattern Recognition (CVPR)*, June 2018, pp. 695–704.
- [15] Y.-T. Wang, X.-L. Zhao, T.-X. Jiang, L.-J. Deng, T.-H. Ma, Y.-T. Zhang, and T.-Z. Huang, “A total variation and group sparsity based tensor optimization model for video rain streak removal,” *Signal Processing: Image Communication*, 2018.
- [16] W. Yang, R. T. Tan, J. Feng, J. Liu, Z. Guo, and S. Yan, “Deep joint rain detection and removal from a single image,” in *2017 IEEE Conference on Computer Vision and Pattern Recognition (CVPR)*, July 2017, pp. 1685–1694.
- [17] L.-J. Deng, T.-Z. Huang, X.-L. Zhao, and T.-X. Jiang, “A directional global sparse model for single image rain removal,” *Applied Mathematical Modelling*, vol. 59, pp. 662 – 679, 2018.
- [18] T.-X. Jiang, T.-Z. Huang, X.-L. Zhao, L.-J. Deng, and Y. Wang, “A novel tensor-based video rain streaks removal approach via utilizing discriminatively intrinsic priors,” in *2017 IEEE Conference on Computer Vision and Pattern Recognition (CVPR)*, July 2017, pp. 2818–2827.
- [19] T.-X. Jiang, T.-Z. Huang, X.-L. Zhao, L.-J. Deng, and Y. Wang, “FastDeRain: A novel video rain streak removal method using directional gradient priors,” *IEEE Transactions on Image Processing*, vol. 28, no. 4, pp. 2089–2102, 2019.
- [20] I. Bayram and M. E. Kamasak, “A directional total variation,” in *2012 Proceedings of the 20th European Signal Processing Conference (EUSIPCO)*, Aug 2012, pp. 265–269.
- [21] R. D. Kongskov and Y. Dong, “Directional total generalized variation regularization for impulse noise removal,” in *Scale Space and Variational Methods in Computer Vision*, François Lauze, Yiqiu Dong, and Anders Bjorholm Dahl, Eds., Cham, 2017, pp. 221–231, Springer International Publishing.
- [22] Y. Wang, J. Yang, W. Yin, and Y. Zhang, “A new alternating minimization algorithm for total variation image reconstruction,” *SIAM Journal on Imaging Sciences*, vol. 1, no. 3, pp. 248–272, 2008.
- [23] D. L. Donoho, “De-noising by soft-thresholding,” *IEEE Transactions on Information Theory*, vol. 41, no. 3, pp. 613–627, May 1995.
- [24] X. Zhao, F. Wang, and M. Ng, “A new convex optimization model for multiplicative noise and blur removal,” *SIAM Journal on Imaging Sciences*, vol. 7, no. 1, pp. 456–475, 2014.
- [25] L. Zhu, C. Fu, D. Lischinski, and P. Heng, “Joint bi-layer optimization for single-image rain streak removal,” in *2017 IEEE International Conference on Computer Vision (ICCV)*, Oct. 2017, vol. 00, pp. 2545–2553.
- [26] X. Fu, J. Huang, X. Ding, Y. Liao, and J. Paisley, “Clearing the skies: A deep network architecture for single-image rain removal,” *IEEE Transactions on Image Processing*, vol. 26, no. 6, pp. 2944–2956, June 2017.
- [27] P. Arbelaez, M. Maire, C. Fowlkes, and J. Malik, “Contour detection and hierarchical image segmentation,” *IEEE Transactions on Pattern Analysis and Machine Intelligence*, vol. 33, no. 5, pp. 898–916, May 2011.